Supplementary Information

Revealing the origin of activity and selectivity of nitrate to ammonia on single transition metal atoms catalysts supported by Ti_2NO_2 monolayer

Yuwen Cheng,[a,b,*] Wenjie Wang, [a] Cuiping Shao,[a]

[a] School of Materials Science and Engineering, Anhui University of Technology, Maanshan 243002, PR China

[b] Anhui Province Key Laboratory of Efficient Conversion and Solid-State Storage of Hydrogen & Electricity, Anhui University of Technology, Maanshan 243002, PR China

[*]Corresponding Authors

E-mail: ywcheng@ahut.edu.cn;

1. Calculation details

1.1 The Gibbs free energy change (Δ*G*) for each element step of NO_3RR

The Gibbs free energy change (ΔG) for each step of NO_3RR are calculated by employing the standard hydrogen electrode (SHE) model, via equation (S1)[1,2]:

$$\Delta G = \Delta E_{DFT} + \Delta E_{ZPE} - T\Delta S \quad (S1)$$

ΔE_{DFT} represents the energy change between the products and reactants, while ΔE_{ZPE} denotes the zero-point energy difference derived from vibrational frequencies, reflecting the entropy change. The temperature (T) is 298K. The catalyst's intrinsic activity hinges on the potential-determining step (PDS), which can be described from maximum Gibbs free energy change (ΔG_{max}) during proton-electron transfer. The PDS allows us to calculate the limiting potential (U_L) with the formula $U_L = - \Delta G_{max}/e$. The ΔZPE-TΔS of intermediates adsorbates are referred from previous works and NIST.[3,4]

1.2 Binding energy

The binding energy (E_b) of TM with Ti_2NO_2 can be evaluated by eq (S2)[5]

$$Eb = E_{TM@Ti_2NO_2} - E_{TM} - E_{Ti_2NO_2} \quad (S2)$$

where $E_{TM@Ti_2NO_2}$, $E_{Ti_2NO_2}$, and E_{TM} represent the total energies of Ti_2NO_2 with and without TM loading, and single TM atom, respectively.

1.3 Adsorption energy of NO_3^-

To avoid calculating the energy of charged NO_3^- directly, gaseous HNO_3 is chosen as a reference based on the following steps.[6-8]

$$HNO_3(g) \rightarrow HNO_3(l) \quad (S3)$$

$$HNO_3(l) \rightarrow H^+ + NO_3^- \quad (S4)$$

$$*+NO_3^- \rightarrow *NO_3 + e \quad (S5)$$

as a result, the NO_3^- adsorption can be described as $*+HNO_3(g) \rightarrow H^+ + *NO_3$. Correspondingly, the adsorption energy of NO_3^- (ΔG^*_{NO3}) can be approximated by

$$\Delta G^*_{NO3} = G^*_{NO3} - G^* - G_{HNO3(g)} + 0.5\Delta G_{H2}(g) \quad (S6)$$

where ΔG^*_{NO3}, G^*, $G_{HNO3(g)}$, ΔG_{H2} are the total energy of TM/Ti_2NO_2 substrates with and without NO_3 adsorption, HNO_3 and H_2 molecules in the gas phase, respectively. $\Delta G_{correct}$ denotes the correction of adsorption energy. According to CRC handbook of chemistry and physics,[9] $\Delta G_{correct}$ is set to 0.392 eV.

1.4 Calculation of charge transfer of TM

The charge transfer (Q_{TM}) of TM is based on Bader charge analysis[10] via equation (S7).

$$Q_{TM} = Q_{bader} - Q_{out} \quad (S7)$$

where Q_{bader} and Q_{out} are the Bader charge via DFT calculation and extranuclear electron of TM.

1.5 Calculation of electronic descriptor (*ψ*)

The electronic descriptor (*ψ*) is a descriptor of NO_3^- reduction properties of NO_3RR, which can be calculated via equation (S8):

$$\psi = \frac{\prod_{i=1}^{N} S_{v}^{2/N}}{(\prod_{i=1}^{N} \chi_i)^{1/N}} \tag{S8}$$

where N is the number of atoms at active centers, S_{v_i} and χ_i are the outmost electron number and electronegativity of the ith atom at active centers, respectively.[11]

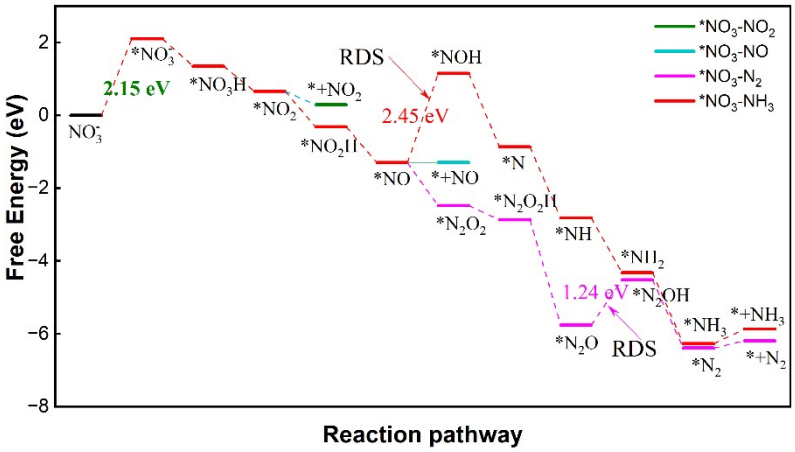

Figure S1. Free energy diagrams for releasing NO_2, NO, N_2, and NH_3 of NO_3RR on Ti_2NO_2.

References

[1] Nørskov J K, Rossmeisl J, Logadottir A, Lindqvist L, Kitchin J R, Bligaard T, Jónsson H. Origin of the overpotential for oxygen reduction at a fuel-cell cathode. *J. Phys. Chem. B*., 2004, **108**, 17886-17892.

[2] Rossmeisl J, Logadottir A, Nørskov J K. Electrolysis of water on (oxidized) metal surfaces. *Chem. Phys.*, 2005, **319**, 178-184.

[3] Niu H, Zhang Z, Wang X, Wan X, Shao C, Guo Y. Theoretical insights into the mechanism of selective nitrate-to-ammonia electroreduction on single-atom catalysts. *Adv. Funct. Mater*., **31**, 2008533.

[4] Computational Chemistry Comparison and Benchmark Database. http://cccbdb.nist.gov/, 2019 (accessed Dec 25, 2019).

[5] Shao C, Wang W, Cheng Y. Synergetic effect of vacancy and dual-metals on defective V_2CO_2 MXene as efficient catalysts for nitrogen reduction reaction. *Appl. Surf. Sci*., 2024, **665**, 160295.

[6] Guo S, Heck K, Kasiraju S, Qian H, Zhao Z, Grabow L C, Miller J T, Wong M S. Insights into nitrate reduction over indium-decorated palladium nanoparticle catalysts. *ACS Catal*., 2018, **8**, 503.

[7] Liu J X, Richards D, Singh N, Goldsmith B. R. Activity and selectivity trends in electrocatalytic nitrate reduction on transition metals. *ACS Catal*., 2019, **9**, 7052.

[8] Calle-Vallejo F, Huang M, Henry J B, Koper M T, Bandarenka A S. Theoretical design and experimental implementation of Ag/Au electrodes for the electrochemical reduction of nitrate. *Phys. Chem. Chem. Phys*., 2013, **15**, 3196.

[9] Lide D R, CRC Handbook of Chemistry and Physics (90th Ed.), 2010.

[10] Henkelman, G.; Arnaldsson, A.; Joń sson, H. A Fast and robust algorithm for Bader decomposition of charge density. *Comput. Mater. Sci.*, 2006, **36**, 354−360.

[11] Gu Y, Wei B, Legut D, Fu Z, Du S, Zhang H, Francisco JS, Zhang R. Single atom modiffed hybrid transition metal carbides as efffcient hydrogen evolution reaction catalysts. *Adv. Funct. Mater.*, 2021, **31**, 2104285.